Journal of The Electrochemical Society, **160** (2) A201-A206 (2013)
0013-4651/2013/160(2)/A201/6/$28.00 © The Electrochemical Society

Lithium Ion Cell Performance Enhancement Using Aqueous $LiFePO_4$ Cathode Dispersions and Polyethyleneimine Dispersant

Jianlin Li,[a,*,z] Beth L. Armstrong,[a] Jim Kiggans,[a] Claus Daniel,[b,c] and David L. Wood, III[a,*]

[a]*Materials Science and Technology Division, Oak Ridge National Laboratory, Oak Ridge, Tennessee 37831-6083, USA*
[b]*Energy and Transportation Science Division, Oak Ridge National Laboratory, Oak Ridge, Tennessee 37831-6083, USA*
[c]*Bredesen Center for Interdisciplinary Research and Graduate Education, University of Tennessee, Knoxville, Tennessee 37996, USA*

Switching manufacturing of composite battery electrodes from an organic system to an aqueous system provides both economic and environmental advantages. However, particle agglomeration of the electrode components and poor wetting of electrode dispersions to the current collectors are inherently introduced. Particle agglomeration can be mitigated by selection of appropriate dispersants. This research examines the effect of dispersant, poly(ethyleneimine) (PEI), on the associated morphology and electrochemical performance of $LiFePO_4$. The addition of PEI reduces the agglomerate size and contributes to a more homogeneous distribution of cathode constituents, which results in a smoother, more uniform cathode surface. The $LiFePO_4$ cathodes with PEI demonstrated a higher Li^+ diffusion coefficient (1×10^{-14} cm^2 s^{-1}), better initial capacity (>142 mAh g^{-1}), greater capacity retention (~100%), and superior rate performance compared to the cathodes without PEI. When PEI concentration was varied, the $LiFePO_4$ cathode with 2 wt% PEI exhibited the best performance at 167 mAh g^{-1} capacity (98% of the theoretical capacity) and 100% retention after 50 cycles when discharged at 0.2C at 25°C in a half cell.
© 2012 The Electrochemical Society. [DOI: 10.1149/2.037302jes] All rights reserved.

Manuscript submitted August 8, 2012; revised manuscript received October 17, 2012. Published November 28, 2012. This was Paper 190 presented at the Montreal, QC, Canada, Meeting of the Society, May 1–6, 2011.

Rechargeable lithium-ion batteries have been applied to electric vehicles (EVs) recently and production of EVs is foreseen to increase substantially in the near future. However, application to EVs is limited by performance and cost.[1] It is essential to develop new processes to manufacture lithium-ion batteries at low cost and with little environmental impact. The key to reducing the cost of lithium-ion batteries lies in utilizing low cost materials and developing low cost material processing[2] since these materials and the associated processing can make up over 70% of cell material cost of lithium-ion cathode.[3]

For conventional lithium-ion batteries, composite cathodes are manufactured through a slurry coating process in which active materials are mixed with additives in a solvent; Poly(vinylidene fluoride) (PVDF) and N-methyl-2-pyrrolidone (NMP) are the typical binder and solvent, respectively. Switching the manufacturing of composite cathodes from an organic system to an aqueous system provides a pathway to reduce cost, in which expensive NMP (>$2.25/L when purchased in large quantity) is replaced with deionized water ($0.015/L). The expensive process for recovering and repurifying of NMP would also be eliminated.[4] Based on a recent internal Oak Ridge National Laboratory (ORNL) processing study (unpublished results), this approach has a potential to save up to 70% in the electrode processing steps, translating to a 12% reduction of the overall battery pack cost. Additionally, replacing PVDF with water soluble binders, such as xanthan gum,[4–6] carboxymethyl cellulose (CMC)[7,8] or styrene-butadiene rubber (SBR)[9] would further reduce the cost.[10] According to Zackrisson et al.,[11] replacing NMP with water in manufacturing of lithium-ion batteries also reduces global warming impact by reducing life cycle emission of CO_2 equivalents from 4400 kg to 3400 kg for a 10 kWh battery. Thus, the overall electrode manufacturing process would become substantially more environmentally benign; consequently, there is growing interest in fabricating composite cathodes through aqueous processing.[4,12–21]

Most efforts in fabrication of composite cathodes of lithium-ion batteries through aqueous processing have been made in two areas: improving the wetting of cathode dispersions on the Al foil substrate[6] and controlling agglomeration in cathode dispersions.[4,14,18,19,22] In our previous work, it was reported that the wetting of aqueous $LiFePO_4$ dispersion on an Al foil substrate was dramatically improved (contact angle between dispersions and Al foil decreasing from 41.8° to 0°) by increasing the substrate's surface energy and polarity via a corona plasma treatment, and the resulting $LiFePO_4$ cathodes exhibited superior performance (~20 mAh g^{-1} improvement).[6] Sisbandini et al., improved $LiFePO_4$ cathode capacity through polyetheramine coating on $LiFePO_4$ particle surface, which enhanced the wettablility of aqueous electrolyte on $LiFePO_4$ particle and protected $LiFePO_4$ from forming Li_3PO_4.[23] Some success has been reported in controlling agglomeration in aqueous cathode dispersions. Porcher et al., chose a non-ionic dispersant (Triton X-100) to improve the dispersion of carbon black.[19] Li et al., used polyacrylic acid (PAA-NH_4)[14] to improve the dispersions of a $LiCoO_2$ composite cathode and poly (4-styrene sulfonic acid) (PSSA)[18] to improve a $LiFePO_4$ composite cathode. Better performance has been observed with the dispersants.

Based on other work from our group,[4] poly(ethyleneimine) (PEI) was selected as the dispersant for $LiFePO_4$ based on the zeta potential results. $LiFePO_4$ exhibited a negative charge on particle surfaces at pH > 4.3 [4] while PEI has been shown to yield a positive charge in aqueous ceramic suspensions at pH < 10.[24] It would be easy for PEI to adsorb on $LiFePO_4$ particle surfaces. The aqueous $LiFePO_4$ dispersions exhibited Newtonian behavior with 1.5 wt% PEI and the agglomerate size was minimized.[4] The distribution of electrode components was also more homogeneous with the addition of PEI. However, those efforts focused on the PEI effect on the stability and rheology of $LiFePO_4$ aqueous dispersions, and the PEI effect on $LiFePO_4$ performance was not discussed. In this work, the positive effects of PEI addition on the $LiFePO_4$ cathode coating morphology and performance will be addressed.

Experimental

$LiFePO_4$ (2–3wt% C, P2, Phostech Lithium Inc.), Super P C45 (Timcal) (C45 hereafter), xanthan gum (Nuts Online) and PEI (M_w = 25,000 g mol^{-1}, Sigma-Aldrich) were the materials used in this study. Molecular structure of PEI is shown in Figure 1. PEI is stable between 2.5 to 4.3V as evidenced by the cyclic voltametry (CV) results in Figure 4. The C45 (BET surface area ~45 m^2 g^{-1}) was used as the carbon black. Xanthan gum is a cheap, nontoxic binder that has been successfully used in lithium-ion batteries.[4–6]

The aqueous $LiFePO_4$ dispersions were prepared with the same procedures as those described in our previous work.[4] The components in all the dispersions were maintained at the following by weight ratio where $LiFePO_4$/C45/PEI/xanthan gum/H_2O = 100/10/0-2.0/2.5/350.

The dispersions were coated ultilizing a custom slot-die coater (Frontier Industrial Technology) on pretreated Al foil and dried in

*Electrochemical Society Active Member.
zE-mail: lij4@ornl.gov

Downloaded on 2015-12-23 to IP 128.219.49.14 address. Redistribution subject to ECS terms of use (see ecsdl.org/site/terms_use) unless CC License in place (see abstract).

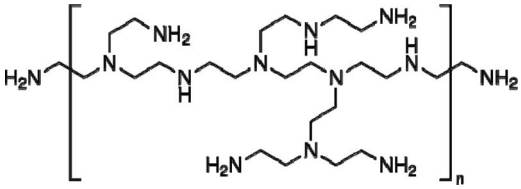

Figure 1. Molecular structure of PEI.

a heating zone consisting of two IR lamps and seven convection ovens. The Al foil was pretreated by corona discharge (Compak 2000, Enrocon) at 1 kW and 10 ft min^{-1} in order to improve its surface energy as discussed previously.[6] The dried cathodes were further dried in a vacuum oven at 90°C for an additional 2 h before being assembled into half cells. The morphology of the dried $LiFePO_4$ green tapes (without secondary vacuum drying) with and without PEI was characterized by a scanning electron microscopy (SEM) (JEOL 6500 FEG-SEM) and an optical microscope (VHX-1000, Keyence).

2032 coin cells were assembled inside a glove box with $LiFePO_4$ and Li metal as the cathodes and counter electrodes, respectively. Celgard 2325 was used as the separator. The cathodes had a loading of 2.5 mg cm^{-2} $LiFePO_4$, and the electrolyte was 1.2 M $LiPF_6$ in ethylene carbonate: diethyl carbonate (3/7 wt ratio, Novolyte). CV experiments were carried out with VSP potentiostats (BioLogic) at 25°C within a scan range of 2.5–4.3 V vs. Li/Li^+ and scan rate of 0.1, 0.2 and 0.5 mV s^{-1}, respectively. The cells were cycled for performance analysis at 0.2C/-0.2C (85 μA cm^{-2}) between 2.5 and 4.2 V vs. Li/Li^+ (VSP, BioLogic) at 25°C. The rate performance was investigated with 0.2C charge rate and varying discharge rate.

Results and Discussion

Morphology of $LiFePO_4$ cathodes.— Figure 2 shows the surface morphology of the $LiFePO_4$ cathodes. There were significant agglomerates, cracks and large pores in the cathode without PEI (Figure 2a). In contrast, the cathodes with PEI exhibited improved morphology with smaller agglomerate size and more uniformly distributed agglomeration, which agrees with the agglomerate size and cathode component distribution results from our previous work.[4] The elimination of these large pores and cracks by adding PEI could beneficially increase the bulk density of the $LiFePO_4$ cathodes. Agglomerate size within the cathode structure also affected the surface roughness as shown in Figure 3. The 3D images of surface morphology of the $LiFePO_4$ cathodes were captured by an optical microscope and the scale bars were synchronized. High surface roughness was found on the

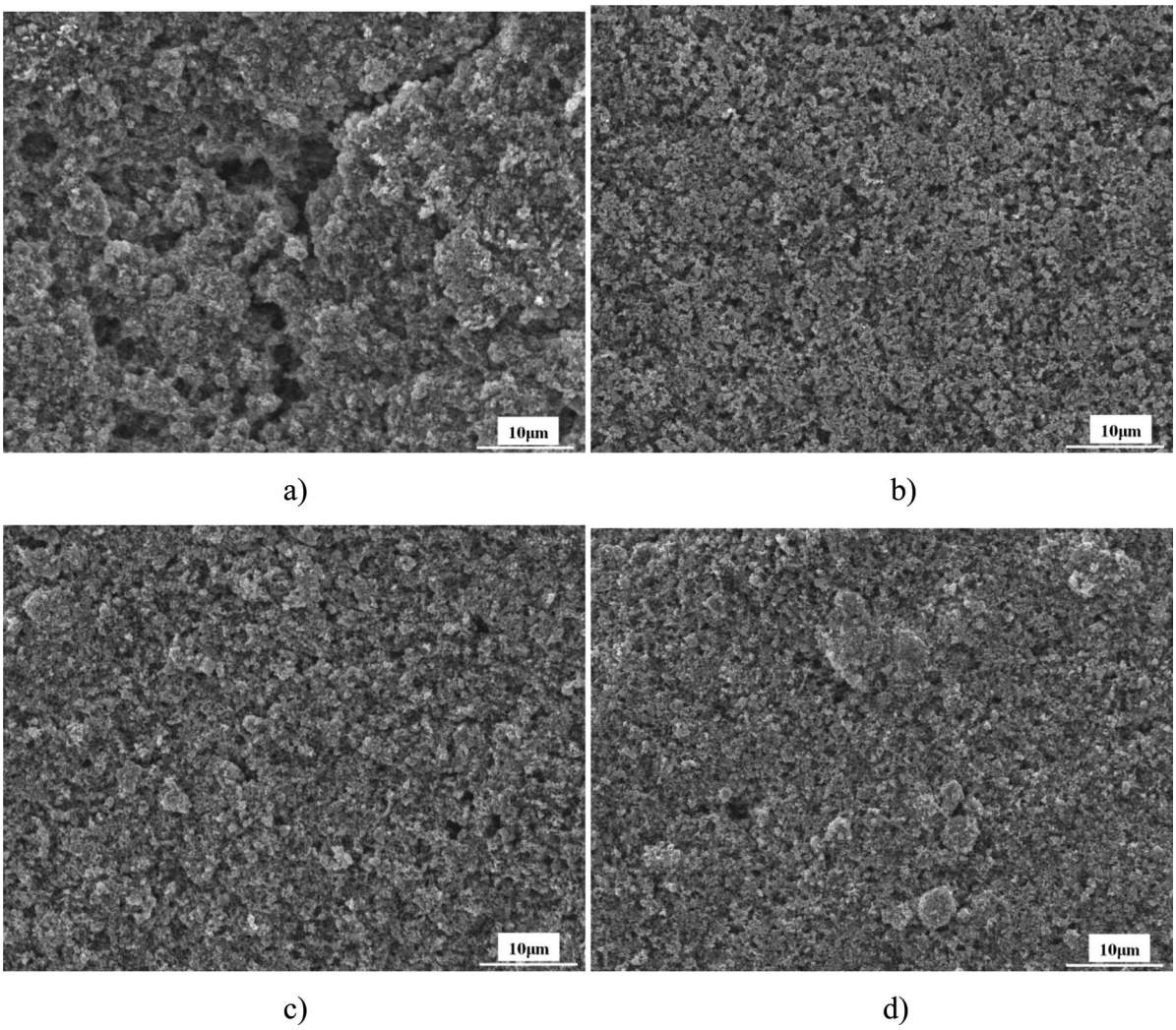

Figure 2. Morphology of $LiFePO_4$ composite cathodes with various PEI concentrations: (a) without PEI; (b) 0.5 wt% PEI; (c) 1.0 wt% PEI and (d) 2.0 wt% PEI. The $LiFePO_4$ cathodes with PEI exhibited smaller agglomerate size and more uniform agglomerate size distribution.

Downloaded on 2015-12-23 to IP 128.219.49.14 address. Redistribution subject to ECS terms of use (see ecsdl.org/site/terms_use) unless CC License in place (see abstract).

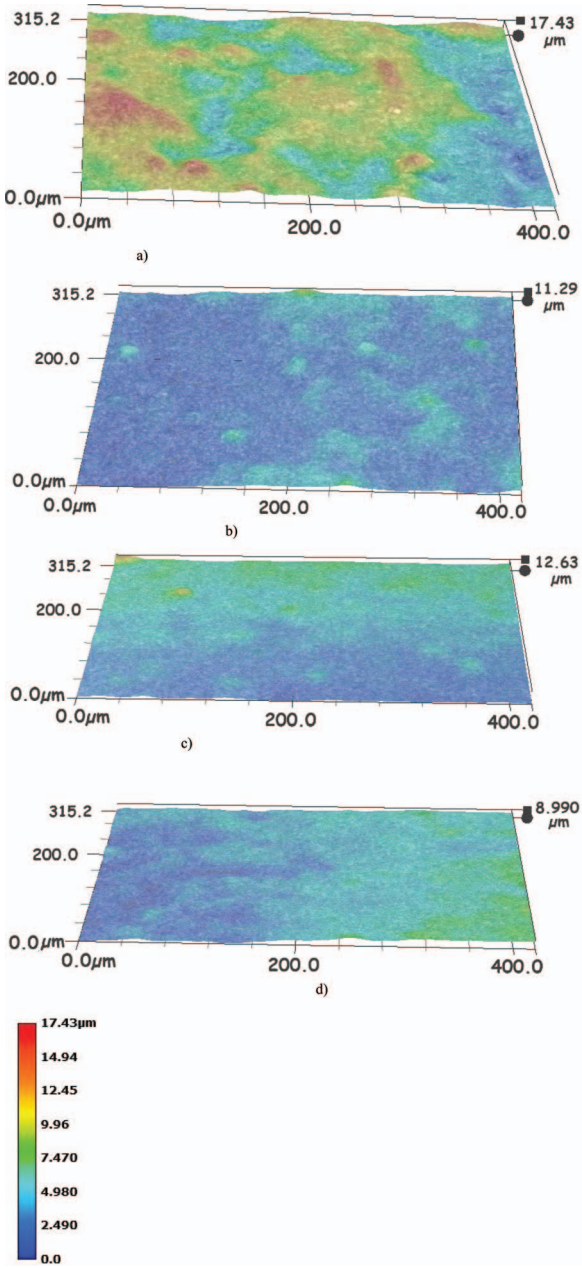

Figure 3. 3D images from optical microscopy of $LiFePO_4$ composite cathode surface with various PEI concentrations: (a) without PEI; (b) 0.5 wt% PEI; (c) 1.0 wt% PEI and d) 2.0 wt% PEI. The $LiFePO_4$ cathodes with PEI demonstrated smoother surface.

cathode without PEI and appeared as "island-like" features. The number of islands dramatically decreased and the color was more uniformed with PEI, indicating much lower surface roughness. These island features were ascribed to large agglomerates, which cause high surface roughness and likely lead to cathode performance degradation. For example, the islands could undergo excessive pressure during electrode calendaring, introducing high mechanical stress to the agglomerate and leading to mechanical fracture and performance degradation. In addition, the islands could exert higher pressure onto the separators during operation, which compromises separator mechanical strength and introduces a safety issue. Furthermore, the high $LiFePO_4$ cathode roughness could increase the distance between electrodes and, consequently, increase the diffusion path length of Li ions resulting in inferior rate performance. Therefore, these potential negative performance and safety effects related to inconsistent agglomerate size and

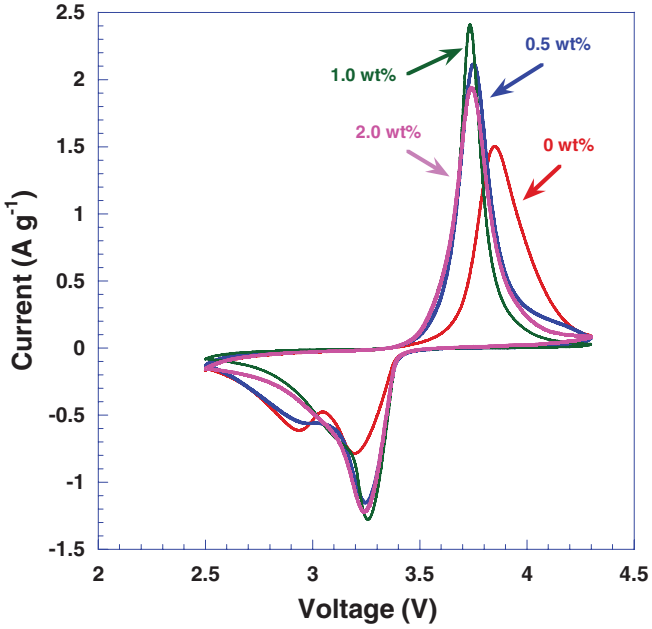

Figure 4. CV scans of $LiFePO_4$ cathodes with various PEI concentrations. The addition of PEI increased current and reduced concentration polarization.

high surface roughness of the $LiFePO_4$ cathode without PEI addition can be mitigated by adding the appropriate amount of PEI into the electrode dispersion. It is noted that there seemed to be a thickness gradient in Figure 3c from top to bottom and (d) from left to right. This was not due to variation in electrode thickness, which was within 1%. Instead, it was attributed to the samples not completed flat and attached to sample holder when the images were taken.

Electrochemical properties of $LiFePO_4$ cathodes.— Figure 4 shows the CV data for the $LiFePO_4$ cathodes with various PEI concentrations on the second cycle at a scan rate of 0.1 mV s^{-1}. There were two anodic peaks in the cathode without PEI. This could be attributed to bimodal distribution in agglomerate size or non-uniform contact between $LiFePO_4$ and carbon black. Larger agglomerate size and/or poor contact between $LiFePO_4$ and carbon black caused lower electronic conductivity,[25] which shifted the anodic peak to lower potential. The peak at ~2.9 V was much less significant than its counterpart, was less pronounced for the cathodes with 0.5 wt% PEI, and disappeared when further increasing PEI concentration. The anodic peak at ~2.9 V for the cathode without PEI was more significant at a higher scan rate as seen in Figure 5, indicating it was related to a diffusion limited process. The disappearance of this anodic peak with PEI addition to the dispersions indicates improved diffusion rate as a result of smaller agglomerate size and more homogeneous distribution of the cathode components. The currents for the cathodic and anodic peaks were different due to the two-phase charge-transfer process during charge and discharge for $LiFePO_4$, in which Li ions were most likely diffusing through regions with $FePO_4$ and $LiFePO_4$.[26–28] The addition of PEI also increased the peak currents. The voltages for the cathodic and anodic peaks are listed in Table I. The separation between redox peaks (ΔV) was 0.65 V for the $LiFePO_4$ cathode without PEI. This large separation indicates significant concentration polarization in this cathode and that the electrochemical behavior was controlled by the Li ion diffusion step. In contrast, the ΔV reduced to ~0.50 V with PEI addition. The smaller ΔV and higher peak currents with PEI addition is ascribed to both the lower ionic resistance of the $LiFePO_4$ solid phase resulted from smaller agglomerates and lower charge-transfer resistance for lithium-ion intercalation and de-intercalation,[16] which results from better dispersion of the carbon black in the cathodes and consequently higher electronic conductivity.

Downloaded on 2015-12-23 to IP 128.219.49.14 address. Redistribution subject to ECS terms of use (see ecsdl.org/site/terms_use) unless CC License in place (see abstract).

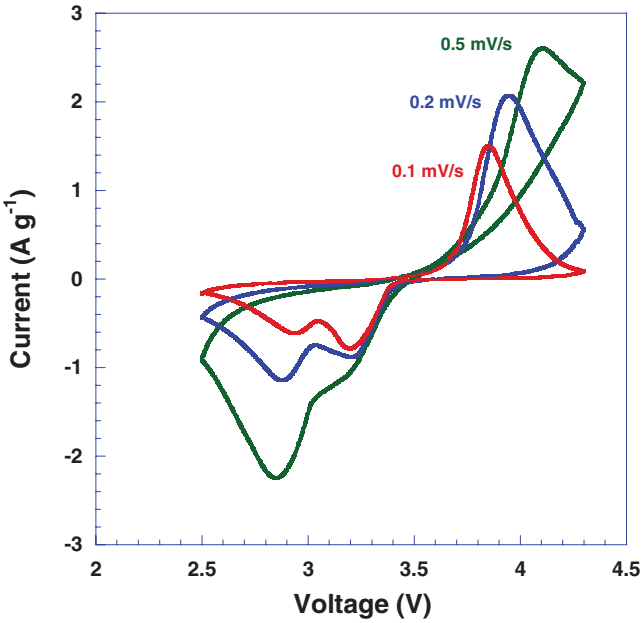

Figure 5. CV curve of $LiFePO_4$ cathode without PEI at various scan rates. The anodic peaks shift to higher voltage with lower scan rate, indicating a diffusion limited process.

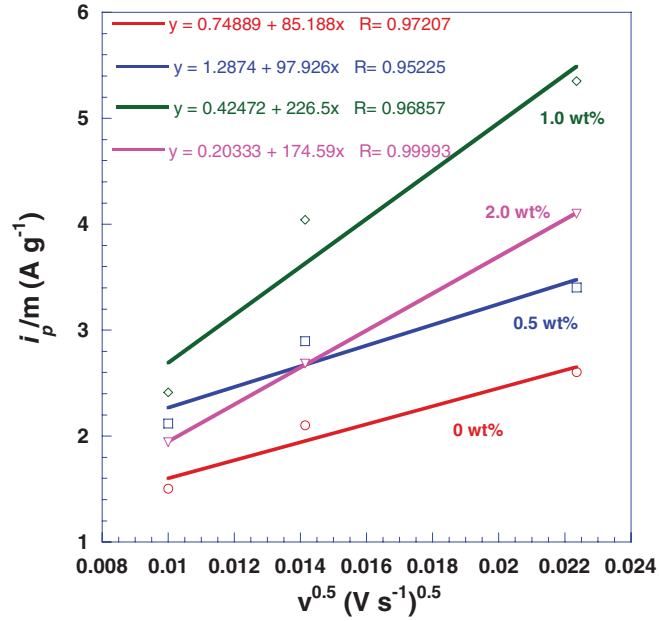

Figure 6. Normalized peak currents versus square root of the scan rates. The normalized peak currents exhibited a linear relationship with respect to the square root of the scan rates, in agreement with Randles-Sevick equation.

CV provides the ability to calculate the Li-ion diffusion coefficient in lithium-ion batteries.[26,29,30] Li intercalation and de-intercalation can be assumed as a reversible reaction and the diffusion coefficient can be described by the Randles-Sevcik equation (for semi-infinite diffusion):[26,31]

$$i_p = 0.4463F\left(\frac{F}{RT}\right)^{1/2} C^* v^{1/2} A D^{1/2} \quad [1]$$

where i_p F, R, T, C^*, v, A and D are the peak current in amperes, the Faraday constant (96485 C mol^{-1}), the universal gas constant (8.314 J mol^{-1} K^{-1}), temperature (K), the initial concentration in mol cm^{-3}, the scan rate in V s^{-1}, the electrode area in cm^2, and the diffusion constant in cm^2 s^{-1}, respectively.

Equation 1 can be rewritten at 25°C as

$$\frac{i_p}{m} = 2.69 \times 10^5 C^*_{Li} v^{1/2} A_e D^{1/2}_{app} \quad [2]$$

where m is the electrode mass in g, C^*_{Li} is the initial concentration of Li in $LiFePO_4$ in mol cm^{-3}, A_e is the electrode area per unit mass in cm^2 g^{-1}, and D_{app} is the apparent diffusion constant of Li-ion in cm^2 s^{-1}. C^*_{Li} is taken as the total amount of Li in a particle before delithiation and is 0.0228 mol cm^{-3} for $LiFePO_4$ since the bulk density and molecular weight of $LiFePO_4$ are 3.6 g cm^{-3} and 157.76 g mol^{-1}, respectively. A_e is taken as the effective area of (010) plane since $LiFePO_4$ has a one-dimensional diffusion path in the (010) direction and it is one-third the total Brunauer-Emmertt-Teller (BET) surface (A_{BET} = 15.1 m^2 g^{-1} here).[26]

Figure 6 shows the plot of $\frac{i_p}{m}$ versus $v^{1/2}$ for the scan rates of 0.1, 0.2 and 0.5 mV s^{-1} (the cathodic peak current is proportional to the square root of scan rate). D_{app} can be calculated from the slope of the linear fit and is also listed in Table I. The addition of PEI significantly increased the Li-ion diffusion coefficient. Maximum D_{app} was obtained at 5.98 × 10^{-14} cm^2 s^{-1} with 1.0 wt% PEI, 7× that without PEI.

Figure 7 shows the half-cell specific capacities of the same $LiFePO_4$ cathodes charged and discharged at 0.2C. Compared to the $LiFePO_4$ cathode without PEI, the ones with PEI addition exhibited higher capacities and the initial specific capacities increased with increasing PEI concentrations, from 142 to 167 mAh g^{-1} (18% improvement) with PEI concentration increasing from 0 wt% to 2 wt%. The cathodes with PEI also demonstrated excellent capacity retention as shown in Figure 8, ~100% after 50 cycles, compared to the 92% for the cathodes without PEI. The capacity retention was over 100% for some cycles, especially for the $LiFePO_4$ cathodes with PEI addition because the capacity increased in the initial cycles, which is common for $LiFePO_4$ cathodes and attributed to the reintercalation of the deintercalated lithium via air and/or water exposure.[32] The $LiFePO_4$ cathode with 2 wt% PEI exhibited the best performance within the PEI concentration range investigated in this work, demonstrating 167 mAh g^{-1} (98% of the theoretical capacity) and 100% retention through 50 cycles when discharged at 0.2C. The improvement in capacities with PEI addition is partially ascribed to the well dispersed com-

Table I. Electrochemical properties from CV measurement at 0.1 mV s^{-1} and Li^+ diffusion constants calculated from Randles-Sevick equation.

PEI%	Cathodic peak Potential (V)	Anodic peak potential (V)	Potential between redox peaks (V)	Peak current (mA mg^{-1})	D_{app}** (×10^{-14} cm^2 s^{-1})
0 wt%	3.84	3.19*	0.65	1.50	0.85
0.5 wt%	3.74	3.24	0.50	2.12	1.12
1.0 wt%	3.73	3.26	0.47	2.41	5.98
2.0 wt%	3.73	3.23	0.50	1.94	3.55

Note: *The anodic peak position was for the higher one.
**The diffusion coefficients were calculated from Figure 6.

Downloaded on 2015-12-23 to IP 128.219.49.14 address. Redistribution subject to ECS terms of use (see ecsdl.org/site/terms_use) unless CC License in place (see abstract).

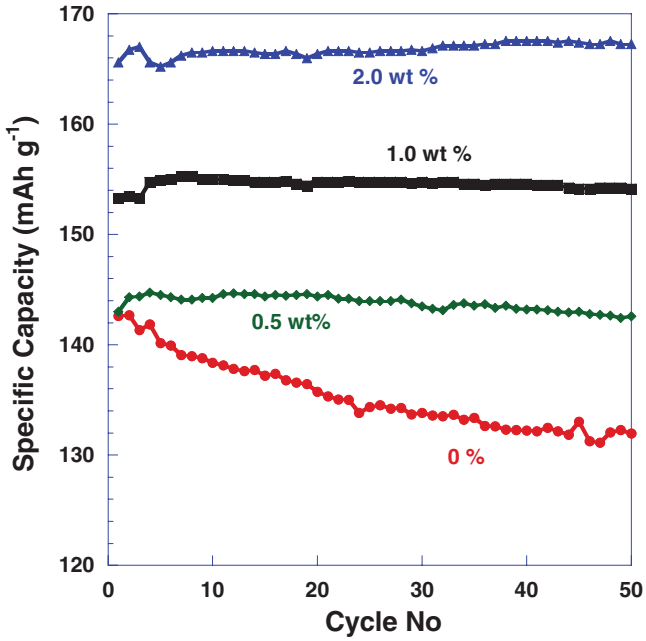

Figure 7. Specific capacities of $LiFePO_4$ cathodes at 0.2C with various PEI concentrations. The addition of PEI increased the cathode capacities.

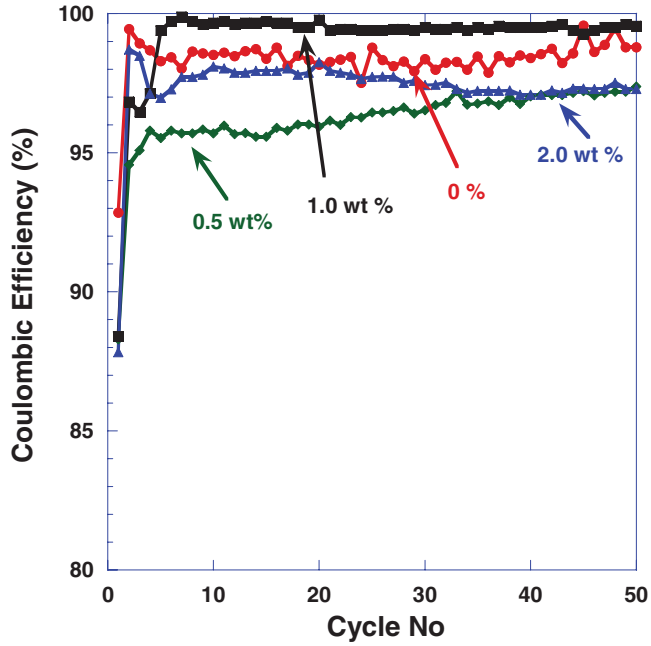

Figure 9. Coulumbic efficiency of $LiFePO_4$ cathodes cycled at 0.2C. $LiFePo_4$ demonstrated good coulumbic efficiency with and without PEI.

ponents in the cathodes improving electronic conductivity. Figure 9 shows the coulombic efficiency of the $LiFePO_4$ cathodes with and without PEI. All electrodes demonstrate excellent coulombic efficiency, above 95% except for the first cycle.

The addition of PEI also improved the rate performance of the $LiFePO_4$ cathodes as evidenced in Figure 10. Higher capacity was observed for the cathodes with PEI than the one without it from C/10 to 1C, and the capacity also increased with increasing PEI concentration. The capacity at C/5 at the end of the rate performance study was essentially identical to that at the beginning, indicating excellent cyclability.

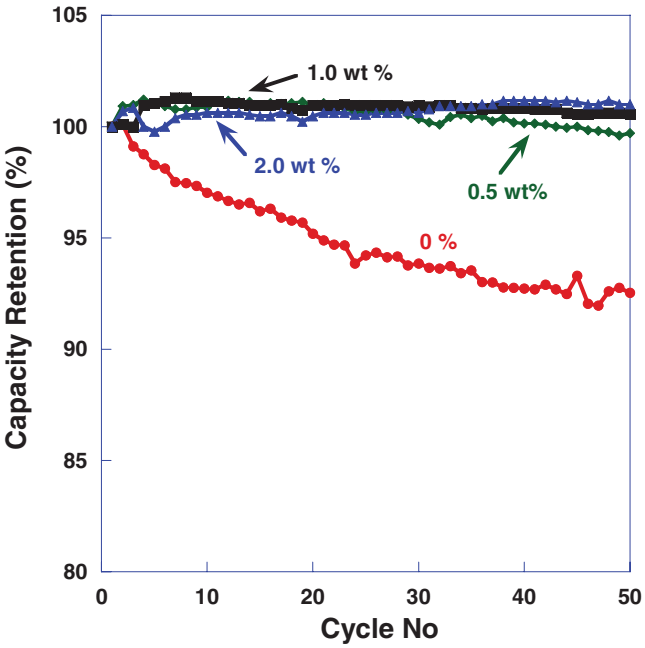

Figure 8. Capacity retention of $LiFePO_4$ cathodes cycled at 0.2C. $LiFePo_4$ demonstrated excellent capacity retention with PEI.

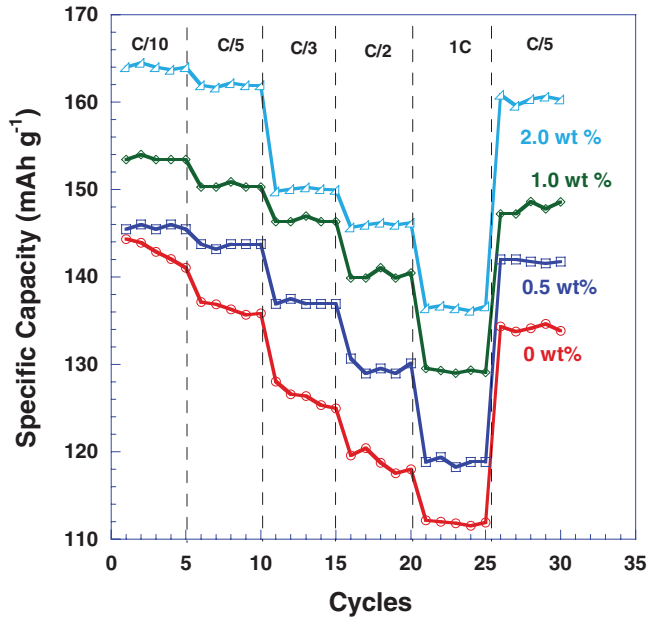

Figure 10. Rate performance of $LiFePO_4$ cathodes. $LiFePO_4$ cathodes exhibited improved rate performance with PEI.

Conclusions

It has been demonstrated that the addition of PEI reduced the agglomerate size and surface roughness of $LiFePO_4$ cathodes. The reduction in the agglomerate size resulted in lower concentration polarization, a higher Li^+ diffusion coefficient and, consequently, better rate performance improvement from both a kinetic and diffusion standpoint. The addition of PEI reduced the concentration polarization of the $LiFePO_4$ cathodes and increased the Li^+ diffusion coefficient. In addition, the capacity of the $LiFePO_4$ cathodes increased with increasing PEI concentration. The $LiFePO_4$ cathode with 2 wt% PEI exhibited the highest capacity, 167 mAh g^{-1} capacity (98% of the theoretical capacity and 16% improvement compared to that without

Downloaded on 2015-12-23 to IP 128.219.49.14 address. Redistribution subject to ECS terms of use (see ecsdl.org/site/terms_use) unless CC License in place (see abstract).

PEI) and 100% retention after 50 cycles when discharged at 0.2C. The addition of PEI also improved the cathode rate performance. PEI is an effective dispersant for aqueous processing of $LiFePO_4$ cathodes.

Acknowledgments

This research was performed at Oak Ridge National Laboratory and was sponsored by the Advanced Manufacturing Office and Vehicle Technologies of the Office of Energy Efficiency and Renewable Energy. Part of the work was conducted at the Shared Research Equipment (SHaRE) user facility, which is sponsored by the ORNL Scientific User Facilities Division. The authors also thank Phostech Lithium Inc. and Timcal Corporation for supplying materials.

References

1. J.-M. Tarascon and M. Armand, *Nature*, **414**, 359 (2001).
2. J. Li, C. Daniel, and D. Wood, *Journal of Power Sources*, **196**, 2452 (2011).
3. J. Gainese and R. Cuenza, "Costs of lithium-ion-batteries for vehicles," Argonne National Laboratory, 2000.
4. J. Li, B. Armstrong, J. Kiggans, C. Daniel, and D. Wood III, *Langmuir*, **28**, 3783 (2012).
5. F. M. Courtel, S. Niketic, D. Duguay, Y. Abu-Lebdeh, and I. J. Davidson, *Journal of Power Sources*, **196**, 2128 (2011).
6. J. Li, C. Rulison, J. Kiggans, C. Daniel, and D. L. Wood III, *J. Electrochem. Soc.*, **159**, A1152 (2012).
7. J.-H. Lee, J.-S. Kim, Y. C. Kim, D. S. Zang, and U. Paik, *Ultramicroscopy*, **108**, 1256 (2008).
8. J.-H. Lee, J.-S. Kim, C. Kim, D. S. Zang, Y.-M. Choi, W. I. Park, and U. Paik, *Electrochemical and Solid-State Letters*, **11**, A175 (2008).
9. J. Orlenius, O. Lyckfeldt, K. A. Kasvayee, and P. Johander, *Journal of Power Sources*, **213**, 119 (2012).
10. S. F. Lux, F. Schappacher, A. Balducci, S. Passerini, and M. Winter, *Journal of the Electrochemical Society*, **157**, A320 (2010).
11. M. Zackrisson, L. Avellán, and J. Orlenius, *Journal of Cleaner Production*, **18**, 1519 (2010).
12. A. Guerfi, M. Kaneko, M. Petitclerc, M. Mori, and K. Zaghib, *Journal of Power Sources*, **163**, 1047 (2007).
13. C.-C. Li, J.-T. Lee, C.-Y. Lo, and M.-S. Wu, *Electrochemical and Solid State Letters*, **8**, A509 (2005).
14. C. C. Li, J. T. Lee, and X. W. Peng, *Journal of the Electrochemical Society*, **153**, A809 (2006).
15. C.-C. Li, J.-T. Lee, Y.-L. Tung, and C.-R. Yang, *Journal of Materials Science*, **42**, 5773 (2007).
16. Z. P. Cai, Y. Liang, W. S. Li, L. D. Xing, and Y. H. Liao, *Journal of Power Sources*, **189**, 547 (2009).
17. W. Porcher, B. Lestriez, S. Jouanneau, and D. Guyomard, *Journal of the Electrochemical Society*, **156**, A133 (2009).
18. C. C. Li, X. W. Peng, J. T. Lee, and F. M. Wang, *Journal of the Electrochemical Society*, **157**, A517 (2010).
19. W. Porcher, B. Lestriez, S. Jouanneau, and D. Guyomard, *Journal of Power Sources*, **195**, 2835 (2010).
20. J.-T. Lee, Y.-J. Chu, F.-M. Wang, C.-R. Yang, and C.-C. Li, *Journal of Materials Science*, **42**, 10118 (2007).
21. J.-T. Lee, Y.-J. Chu, X.-W. Peng, F.-M. Wang, C.-R. Yang, and C.-C. Li, *Journal of Power Sources*, **173**, 985 (2007).
22. J.-H. Lee, U. Paik, V. A. Hackley, and Y.-M. Choi, *Journal of Power Sources*, **161**, 612 (2006).
23. C. Sisbandini, D. Brandell, T. Gustafsson, and L. Nyholm, *Journal of the Electrochemical Society*, **156**, A720 (2009).
24. G. H. Kirby, K. M. Cooley, and B. L. Armstrong, Asme. Tailored rheological behavior of mullite and bsas suspensions using a cationic polyelectrolyte. In *Proceedings of the ASME Turbo Expo 2005*, Vol 1, 2005; pp. 307.
25. C. Fongy, S. Jouanneau, D. Guyomard, J. C. Badot, and B. Lestriez, *Journal of the Electrochemical Society*, **157**, A1347 (2010).
26. D. Y. W. Yu, C. Fietzek, W. Weydanz, K. Donoue, T. Inoue, H. Kurokawa, and S. Fujitani, *Journal of the Electrochemical Society*, **154**, A253 (2007).
27. A. K. Padhi, K. S. Nanjundaswamy, and J. B. Goodenough, *Journal of the Electrochemical Society*, **144**, 1188 (1997).
28. V. Srinivasan and J. Newman, *Journal of the Electrochemical Society*, **151**, A1517 (2004).
29. M. D. Levi and D. Aurbach, *Journal of Electroanalytical Chemistry*, **421**, 79 (1997).
30. G. Leftheriotis, S. Papaefthimiou, and P. Yianoulis, *Solid State Ionics*, **178**, 259 (2007).
31. A. J. Bard and L. R. Faulkner, *Eletrochemical Methodes*; John Wiley & Sons, Inc.: New York, 1980.
32. J. F. Martin, A. Yamada, G. Kobayashi, S. I. Nishimura, R. Kanno, D. Guyomard, and N. Dupre, *Electrochemical and Solid State Letters*, **11**, A12 (2008).

Downloaded on 2015-12-23 to IP **128.219.49.14** address. Redistribution subject to ECS terms of use (see **ecsdl.org/site/terms_use**) unless CC License in place (see abstract).